Dalton Transactions

Accepted Manuscript

This article can be cited before page numbers have been issued, to do this please use: W. Lee, T. Hsu, W. Hung and J. Fang, *Dalton Trans.*, 2019, DOI: 10.1039/C9DT01339C.




ROYAL SOCIETY OF CHEMISTRY

rsc.li/dalton

View Article Online
DOI: 10.1039/C9DT01339C

COMMUNICATION

# Copper(II)–dipicolylamine–coumarin sensor for maltosyltransferase assay

Received 00th January 20xx,
Accepted 00th January 20xx

DOI: 10.1039/x0xx00000x

Wei-Li Lee,[a,‡] Tse-Wei Hsu,[a,‡] Wei-Cheng Hung,[a] and Jim-Min Fang*[ab]

**A Cu(II)–[di(2-methylpyridyl)methylamino]coumarin fluorescence turn-on sensor (Cu-1b) is designed to detect phosphate ion with $K_{ass}$ = 1.4 × 10$^5$ M$^{-1}$ in HEPES buffer. Cu-1b is applied to probe the GlgE catalyzed maltose-transfer reaction of α-maltose-1-phosphate to α-1,4-glucan with concomitant release of phosphate ion in *Mycobacterium tuberculosis*.**

Tuberculosis (TB) is a serious infectious disease caused by *Mycobacterium tuberculosis* (*Mtb*), which has persistently evolved to multi- and extensively-drug resistant strains. The maltosyltransferase GlgE is recently validated as an appealing anti-TB target.[1] GlgE uses α-maltose-1-phosphate (M1P) as the substrate for elongation of α-1,4-glucan with concomitant release of phosphate ion (Pi).[2] Inhibition of GlgE causes accumulation of M1P, and triggers the self-poisoning of *Mtb*. GlgE is essential for the survival of *Mtb*, but absent in human body. The activity of GlgE can be monitored by quantitative analysis of the released Pi (Figure 1). An MESG-based phosphate assay kit is commonly applied to quantify the released Pi by colorimetric method.[3–5] MESG is converted by purine nucleoside phosphorylase (PNP) in the presence of Pi to give AMMP with the absorption band shifting from 330 nm to 360 nm. The difference of 360-nm absorbance between MESG substrate and AMMP product varies depending on the pH of media.[5] Thus, the MESG-based phosphate assay may give inaccurate results under certain conditions due to pH change in the enzymatic reactions. Though the aminium ion in MESG is a crucial moiety for acting as a good PNP substrate, the positively charged moiety also causes thermal instability of nucleoside, especially in basic media.[5] To overcome the limitation on using MESG-based phosphate assay, we thus exploited a new fluorescent turn-on sensor Cu-**1b** that can selectively detect Pi over M1P in buffer solution. It is noted that Pi in extracellular environment (pH 7.4) exists as equilibrium of hydrogen phosphate ($HPO_4^{2-}$) and dihydrogen phosphate ($H_2PO_4^-$).

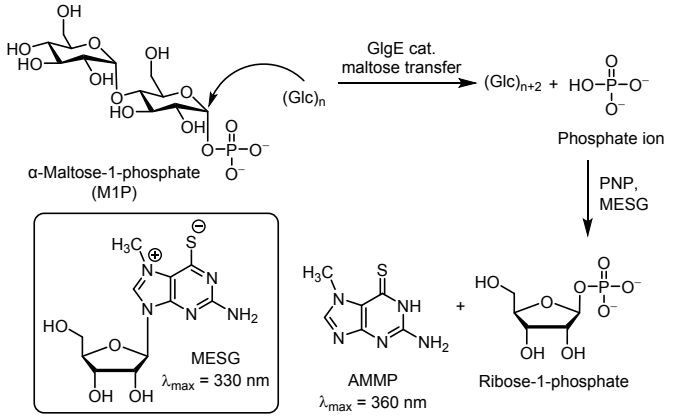


**Figure 1.** GlgE catalyzed elongation of α-1,4-glucan with α-maltose-1-phosphate in *M. tuberculosis*. The released phosphate ion is quantified using an MESG assay kit via the PNP catalyzed phospho-transfer reaction.

Our designed ligand **1b** comprises a coumarin fluorophore that is attached to a di(methylpyridylmethyl)amine (mDPA) moiety for chelation with Cu(II) ion as the binding site of Pi (Figure 2, R = Me). The fluorescence of **1b** will be dimmed by chelation with metal ion, and turned bright when the chelation strength of mDPA–metal motif is attenuated by addition of negatively charged Pi. The sensor operated by internal charge transfer (ICT) is expected to be sensitive to Pi and less susceptible to solvent effect. Furthermore, Cu-**1b** complex having methyl substituents at the *ortho* position of each pyridine ring[6] is expected to provide steric hindrance to disfavor the binding with bulky M1P. To demonstrate the important role of the methyl substituents, the related Cu(II)–DPA–coumarin complex (Cu-**1a**) was also examined.

Various molecular fluorescent sensors have been devised to detect phosphate ion, diphosphate ion (PPi) and biological phosphates.[7–13] Metal complexes appear to be good candidates for operation in water and biological media. The chemosensors bearing $Zn^{2+}$–DPA or $Cu^{2+}$–DPA motif have been

[a] *Department of Chemistry, National Taiwan University, Taipei 106, Taiwan. E-mail: jmfang@ntu.edu.tw*
[b] *The Genomics Research Centre, Academia Sinica, Taipei 115, Taiwan.*
† Footnotes relating to the title and/or authors should appear here.
Electronic Supplementary Information (ESI) available: Experimental procedures, UV-vis, fluorescence, ESI–MS and NMR spectra, Job plots and X-ray crystallographic data (CCDC 1876683). See DOI: 10.1039/x0xx00000x

View Article Online
DOI: 10.1039/C9DT01373G

exploited to detect various anions,[14–16] for example, Yoon and coworkers have shown that some $Cu^{2+}$–DPA–coumarin complexes can selectively bind with PPi over Pi, AMP, ADP and ATP.[17] Kikuchi and coworkers have designed a chemosensor which contains an azacycle linked to coumarin for complexation with $Cd^{2+}$ ion to probe PPi in HEPES buffer.[18] Nonetheless, this sensor exhibits much weaker affinity to Pi.[18] Glass and coworkers have devised a ditopic sensor, which features a coumarin aldehyde for iminium formation to assist the $Zn^{2+}$–DPA unit in chelation with phosphoserine.[19] Hamachi and coworkers have demonstrated a glycosyltransferase assay by utilizing antracene-9,10-bis(DPA–$Zn^{2+}$) complex,[20] which selectively binds uridine diphosphate (UDP) over galactosyl-UDP.

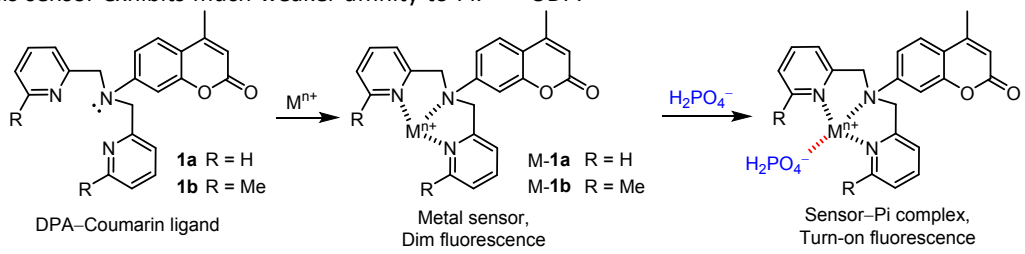


**Figure 2.** Ligand **1b** derived from merge of di(methylpyridylmethyl)amine (mDPA) with coumarin, and the corresponding DPA–coumarin ligand **1a**. Fluorescence dims on formation of metal–ligand complex, and turns bright on binding with negatively charged phosphate ion via an ICT mechanism.

Scheme 1 shows the synthetic procedures of ligands **1a** and **1b**. The alkylation reaction of *m*-silyloxyaniline (**2**) with two equivalents of 2-(bromomethyl)pyridine (**3a**) was accompanied by in situ removal of the silyl protecting group to give the DPA–phenol product **4a**. Using *m*-aminophenol for direct alkylation with **3a** (2 equiv) was complicated by *O*-alkylation to give an inferior yield of **4a** (< 30%). By a similar procedure, alkylation of *m*-silyloxyaniline with 2-bromomethyl-6-methylpyridine (**3b**) afforded **4b**, which underwent Pechmann condensation with ethyl acetoacetate to give ligand **1b**.

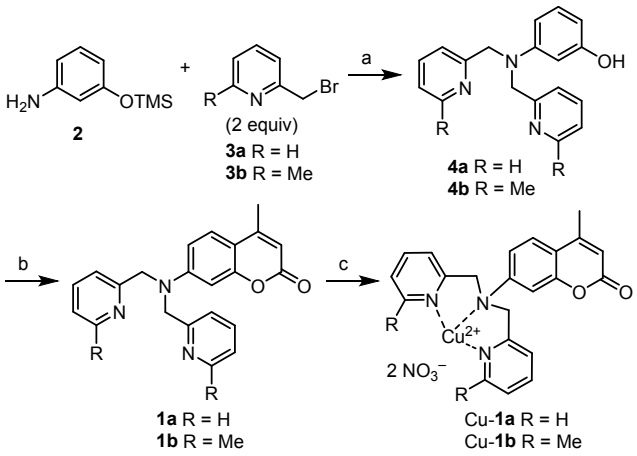


**Scheme 1.** Synthesis of DPA–coumarin ligands (**1a** and **1b**) and their copper(II) complexes. *Reagents and reaction conditions*: (a) $NaOH_{(aq)}$, CTAC, rt, 24–48 h; **4a**, 55%; $NaHCO_{3(aq)}$, CTAC, rt, 24–48 h; **4b**, 66%. (b) ethyl acetoacetate, 70% $H_2SO_{4(aq)}$, rt, 3 h; **1a**, 94%; **1b**, 90%. (c) $Cu(NO_3)_2$, MeOH, $H_2O$, 30 min. CTAC = cetyltrimethylammonium chloride.

Ligand **1b** exhibited an absorption maximum at 358 nm and a strong fluorescence emission at 442 nm in MeOH solution. The broad fluorescence band with a large Stokes shift indicated that an ICT mechanism involved in the fluorescence emission.[21, 22] After screening various metal ions (supplementary Figure S1), $Cu^{2+}$ ion was found to cause the most prominent chelation-enhanced quenching effect in fluorescence,[23, 24] Formation of Cu-**1b** complex also showed a significant blue shift of absorption band from 358 nm to 328 nm (Figure 3).

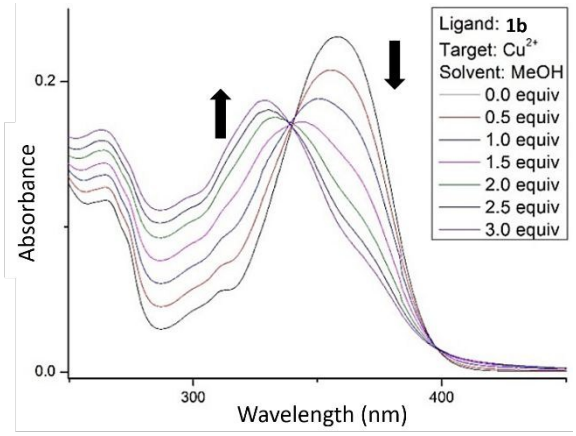


**Figure 3.** UV-vis titration curve of ligand **1b** (10 μM solution in MeOH) upon incremental additions of $Cu^{2+}$ ions (10 mM stock solution in water).

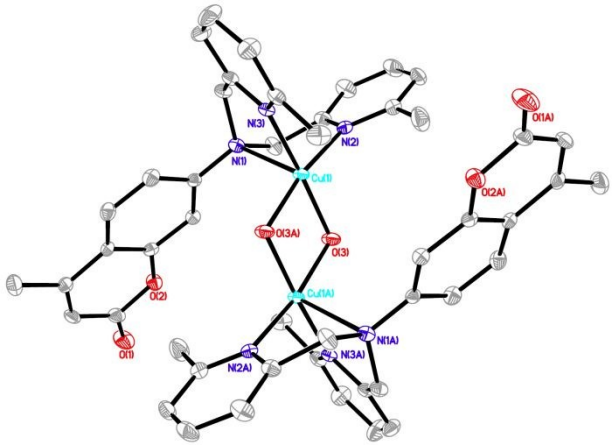

**Figure 4.** ORTEP drawing of Cu-**1b** complex in the dimeric form $[H_2O•Cu\text{-}1b]_2$ (CCDC 1876683); thermal ellipsoids drawn at the 50% probability level.

The UV-vis titration curves exhibited an isosbestic point at 339 nm, indicating the complex of Cu-**1b** was formed in 1:1 stoichiometry that was also confirmed by Job plot (supplementary Figure S2D). In the ESI–HRMS spectrum, a

View Article Online
DOI: 10.1039/C9DT01339C



signal at *m/z* 510.0949 was attributable to the $[(Cu\text{-}\mathbf{1b})\bullet NO_3]^+$ ion. The X-ray diffraction of the crystal obtained from aqueous MeOH indicated the existence of a dimeric $[H_2O\bullet Cu\text{-}\mathbf{1b}]_2$ complex with two water molecules coordinated to the two Cu(II) centers (Figure 4).

In comparison, the UV-vis titration curves of ligand **1a** with $Cu^{2+}$ ion did not exhibit an isosbestic point (supplementary Figure S2A). The Job plot showed the maximum at 0.4 molar ratio (supplementary Figure S2B), which could be ascribed to the combination of Cu-**1a** and **1a**-Cu-**1a** complexes at equilibrium. As the 1:1 stoichiometry of Cu-**1b** was clearly defined, it was chosen to investigate the binding events with Pi and M1P. Upon incremental addition of Pi to Cu-**1b** in MeOH solution, the absorption at 358-nm gradually increased at the expense of the 328-nm absorption of Cu-**1b** (supplementary Figure S3A). As that depicted in Figure 2, coordination of phosphate ion reduced the mDPA–$Cu^{2+}$ chelation strength, and thus caused a bathochromic shift of the absorption band. The binding of Cu-**1b** with Pi also rendered appreciable enhancement of the fluorescence at 442 nm, which reached saturation upon addition of 1.5 equiv Pi (supplementary Figure S3B). The association constant ($K_{ass}$) was calculated to be (6.2 ± 0.1) × $10^6$ $M^{-1}$ in MeOH based on 1:1 stoichiometry for the Pi•(Cu-**1b**) complexation. The 1:1 complex of Pi•(Cu-**1b**) was supported by the ESI–HRMS analysis, which showed a signal at *m/z* 566.8617 attributable to the sodiated Pi•(Cu-**1b**) ion $[C_{24}H_{24}CuN_3O_6P+Na]^+$ (supplementary Figure S6).

To cope with GlgE assay that is generally performed in buffer solution, we also studied the photochemical properties of Cu-**1b** sensor in HEPES buffer. Ligand **1b** and Cu-**1b** complex exhibited the absorption bands at 364 and 334 nm in HEPES buffer (pH 7.4), respectively. Upon addition of phosphate ion, formation of the Pi•(Cu-**1b**) complex was characterized by showing the isosbestic point at $\lambda_{abs}$ = 343 nm (Figure 5A). The binding of phosphate ion to Cu-**1b** also enhanced the fluorescence intensity at 448 nm (Figure 5B). The 1:1 stoichiometry of Pi•(Cu-**1b**) complex in HEPES buffer was verified by Job plot (supplementary Figure S4C). The $K_{ass}$ value of (1.4 ± 0.2) × $10^5$ $M^{-1}$ in HEPES buffer was determined from the fluorescence titration (supplementary Figure S4A). The changes of fluorescence intensity on binding of Cu-**1b** with Pi at low concentrations (e.g. 1–10 μM) exhibited a good linear relationship, and are suitable for quantitation of Pi in physiological condition (supplementary Figure S4B). The limit of detection (LOD) is 2.08 × $10^{-6}$ M. It was noted that the intensity of absorption and fluorescence throughout the titration process of Cu-**1b** with Pi could not revert to the original absorption or fluorescence intensity of free ligand **1b** at $\lambda_{abs}$ = 364 nm and $\lambda_{em}$ = 448 nm, respectively. Thus, addition of Pi to Cu-**1b** likely forms the Pi•(Cu-**1b**) complex, rather than abstracts $Cu^{2+}$ ion from Cu-**1b** to release free ligand **1b**.

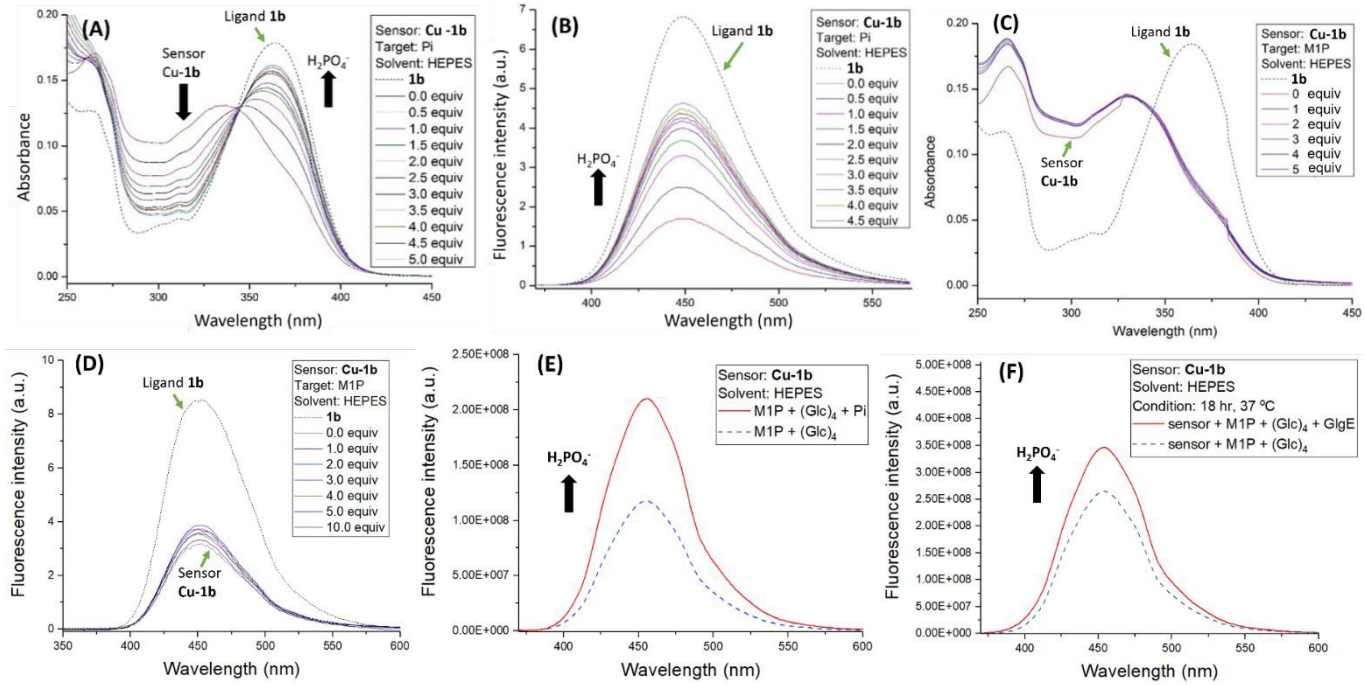


**Figure 5.** Titration curves of sensor Cu-**1b** ($10^{-5}$ M) in HEPES buffer (pH 7.4): (A & B) Incremental additions of Pi; and (C & D) incremental additions of M1P. (E) Fluorescence enhancement by addition of Pi to a solution of M1P (1.0 × $10^{-4}$ M) and maltotetraose (1.25 × $10^{-4}$ M) in HEPES buffer (20 mM, pH 7.53, containing 10 mM $MgCl_2$). (F) Detection of GlgE catalyzed reaction in HEPES buffer (20 mM, pH 7.53, containing 10 mM $MgCl_2$) by fluorescence enhancement. $\lambda_{ex}$ = 343 nm, $\lambda_{em}$ = 448 nm.

The Cu-**1b** sensor was insensitive to halide, acetate and sulfate ions in HEPES buffer, but bound with diphosphate ion (supplementary Figure S5). To our anticipation, Cu-**1b** could not effectively bind with M1P as no appreciable change of the absorption or fluorescence was observed (Figure 5C and 5D). In contrast, enhanced fluorescence was observed by addition of Pi (1.0 × $10^{-4}$ M) to an HEPES solution containing M1P (1.0 × $10^{-4}$ M), maltotetraose (1.25 × $10^{-4}$ M) and Cu-**1b** (1.0 × $10^{-5}$ M) (Figure 5E). Compared with the strong binding of Pi, the access of M1P bearing a bulky maltosyl group to Cu-**1b** would

be blocked by the methyl substituents on the pyridine rings. When M1P ($1.0 \times 10^{-4}$ M) and maltotetraose ($1.0 \times 10^{-4}$ M) were incubated with GlgE (47.5 μg) and Cu-**1b** ($1.0 \times 10^{-5}$ M) in HEPES buffer for 18 h at 37 °C, the fluorescence at 448 nm increased as Pi was released from the enzymatic reaction (Figure 5F).

In summary, we have developed a coumarin based Cu(II)−mDPA sensor (Cu-**1b**) using ICT as the sensing mechanism for selective detection of phosphate ion in HEPES buffer with an association constant of $1.4 \times 10^5$ $M^{-1}$. Upon binding with phosphate ion, the dim sensor Cu-**1b** turns bright. Our experimental results indicate that the sensing event is consistent with formation of Pi•(Cu-**1b**) complex, rather than abstraction of $Cu^{2+}$ ion from Cu-**1b** to release free ligand **1b**. The methyl substituents introduced to the *ortho*-positions of the pyridine rings in the DPA moiety not only enhance the metal–ligand binding strength but also provide steric hindrance to prevent the access of bulky maltose-1-phosphate. We also demonstrate that the Cu(II)−mDPA−coumarin sensor acts as a robust and sensitive sensor to probe the GlgE catalyzed reaction. This fluorescence turn-on assay may facilitate the screening of GlgE inhibitors for discovery of new anti-TB drugs.

This research was supported by Academia Sinica and Ministry of Science and Technology [MOST 103-2113-M-002-017-MY3, MOST 106-0210-01-15-02, and MOST 107-0210-01-19-01]. We thank Mr. Tzu-Hsien Tseng at the Department of Chemistry, National Chung Hsing University for X-ray crystallographic analysis.

## Conflicts of interest

There are no conflicts to declare.

## Notes and references

‡ W.-L. L and T.-W. H contributed equally.

1 R. Kalscheuer, K. Syson, U. Veeraraghavan, B. Weinrick, K. E. Biermann, Z. Liu, J. C. Sacchettini, G. Besra, S. Bornemann, and W. R. Jacobs, *Nat. Chem. Biol.* 2010, **6**, 376.
2 K. Syson, C. E. Stevenson, A. M. Rashid, G. Saalbach, M. Tang, A. Tuukkanen, D. I. Svergun, S. G. Withers, D. M. Lawson S. Bornemann, *Biochemistry* 2014, **53**, 2494.
3 M. R. Webb, *Proc. Natl. Acad. Sci. U.S.A.* 1992, **89**, 4884.
4 S. K. Veleti, J. J. Lindenberger, D. R. Ronning and S. J. Sucheck, *Bioorg. Med. Chem.* 2014, **22**, 1404.
5 S. K. Veleti, J. J. Lindenberger, S. Thanna, D. R. Ronning and S. J. Sucheck, *J. Org. Chem.* 2014, **79**, 9444.
6 C.-T. Chen, C.-L. Chiang, Y.-C. Lin, L.-H. Chan, C.-H. Huang, Z.-W. Tsai and C.-T. Chen, *Org. Lett.* 2003, **5**, 1261.
7 A. P. de Silva, H. Q. N. Gunaratne, T. Gunnlaugsson, A. J. M. Huxley, C. P. McCoy, J. T. Rademacher and T. E. Rice, *Chem. Rev*. 1997, **97**, 1515.
8 R. Martínez-Máñez and F. Sancenón, *Chem. Rev.* 2003, **103**, 4419.
9 S. K. Kim, D. H. Lee, J. I. Hong and J. Yoon, *Acc. Chem. Res.* 2009, **42**, 23.
10 A. E. Hargrove, S. Nieto, T. Zhang, J. L. Sessler and E. V. Anslyn, *Chem. Rev.* 2011, **111**, 6603.
11 D. Zhang, J. R. Cochrane, A. Martinez and G. Gao, Recent advances in $H_2PO_4^-$ fluorescent sensors. *RSC Adv*. 2014, **4**, 29735.
12 P. A. Gale and C. Caltagirone, *Chem. Soc. Rev.* 2015, **44**, 4212.
13 J. Wongkongkatep, A. Ojida and I. Hamachi, *Top. Curr. Chem*. 2017, **375**, 30.
14 E. J. O'Neil and B. D. Smith, *Coord. Chem. Rev*. 2006, **250**, 3068.
15 T. Sakamoto, A. Ojida and I. Hamachi, *Chem. Commun.* 2009, 141.
16 H. T. Ngo, X. Liu and K. A. Jolliffe, *Chem. Soc. Rev.* 2012, **41**, 4928.
17 M. J. Kim, K. M. K. Swamy, K. M. Lee, A. R. Jagdale, Y. Kim, S.-J. Kim, K. H. Yoo, J. Yoon, *Chem. Commun*. 2009, 7215.
18 S. Mizukami, T. Nagano, Y. Urano, A. Odani and K. Kikuchi, *J. Am. Chem. Soc.* 2002, **124**, 3920.
19 C. M. Cooley, K. S. Hettie, J. L. Klockow, S. Garrison and T. E. Glass, *Org. Biomol. Chem.* 2013, **11**, 7387.
20 J. WongKongkatep, Y. Miyahara, A. Ojida and I. Hamachi, *Angew. Chem. Int. Ed*. 2006, **45**, 665.
21 X. Peng, Y. Xu, S. Sun, Y. Wu and J. Fan, *Org. Biomol. Chem.* 2007, **5**, 226.
22 W. Goodall and J. A. G. Williams, *Chem. Commun*. 2001, 2514.
23 M. C. Morris, Ed., Progress in Molecular Biology and Translational Science, Vol. 113, Fluorescence-based biosensors: from concepts to applications. Academic press: Oxford, UK, 2013.
24 R. Bergonzi, L. Fabbrizzi, M. Licchelli and C. Mangano, *Coord. Chem. Rev*. 1998, **170**, 31.

## Table of Contents

View Article Online
DOI: 10.1039/C9DT01339C

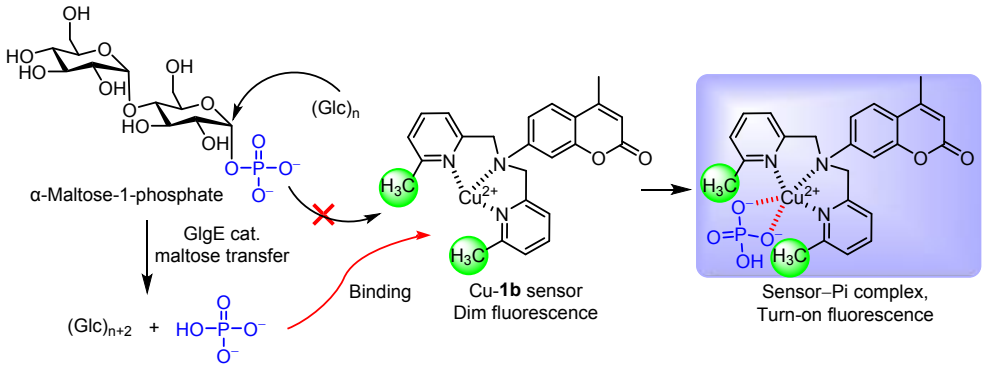


A fluorescence turn-on sensor (Cu-**1b**) is designed for selective detection of the phosphate ions released from GlgE catalyzed maltose-transfer reaction.